

# THE USE OF FINITE ELEMENTS METHOD FOR ANALYZING THE LOAD OCCURRING IN COMPONENTS OF ENDOPROSTHESES

## WYKORZYSTANIE METODY ELEMENTÓW SKOŃCZONYCH DO ANALIZY OBCIĄŻEŃ WYSTĘPUJĄCYCH W KOMPONENTACH ENDOPROTEZ

Michał Sobociński\*, Marcin Nabrdalik

Politechnika Częstochowska, Wydział Inżynierii Mechanicznej i Informatyki, Instytut  
Technologii Mechanicznych, 42-201 Częstochowa, al. Armii Krajowej 21

\*e-mail: sobocinski@iop.pcz.pl

### ABSTRACT

This paper presents numerical analysis of strength in virtual hip and knee joints by means of the finite elements method FEM. Predicting the places in implants, where damage or premature wear may occur, is extremely important. The obtained results helped to exhibit weak points in examined models, and thus may be used to protect premature wear of endoprosthesis elements. The numerical analysis was based on the finite elements method FEM using Autodesk Simulation Mechanical 2016 software and the ADINA 7.5.1.

**Keywords:** endoprosthesis, FEM, contact stress

### STRESZCZENIE

Celem pracy była numeryczna analiza wytrzymałościowa zmian w wirtualnym stawie biodrowym i kolanowym. Zastosowano metodę elementów skończonych. Zastosowanie rozwiązań analitycznych mających na celu wykazanie możliwych miejsc w modelu, gdzie dochodzić może do uszkodzeń lub przedwczesnego zużycia współpracujących elementów, jest niezmiernie ważne. Otrzymane wyniki uwiaryściły takie miejsca, a tym samym mogą być wykorzystane do przeciwdziałania skutkom wynikającym z przedwczesnego zużycia elementów endoprotezy. Analiza numeryczna została wykonana w oparciu o metodę elementów skończonych przy wykorzystaniu oprogramowania Autodesk Simulation Mechanical 2016 oraz ADINA 7.5.1.

**Słowa kluczowe** endoproteza, metoda elementów skończonych, naprężenia kontaktowe

### 1. Introduction

Analytical solutions aimed at indicating the areas where damages or premature wear of cooperating elements in endoprostheses may occur, are very important. Majority of mechanical failures in alloplasty are caused by material fatigue. To reduce the risk, we can either increase the fatigue resistance of the

material or decrease the load strain. All presented numerical calculations allow to demonstrate the influence of some parameters of endoprostheses on the values of stress and strain in polyethylene inserts.

Some tests proved that the weakest point of endoprosthesis is a polyethylene insert [1, 2]. All the approved solutions, as so far, were based on simplified models [3, 4]. The very direct application of load models of hip and knee joints do not precisely reflect the real load features [5, 6, 7, 8]. The use of specific modular endoprosthesis requires more thorough analysis of additional contact points in such system, with the emphasis on technological conditions.

From the other side, replaceable polyethylene elements in knee joint endoprostheses allow to decrease the number of inspection treatments. The numerical analysis presented hereby is the fast and reliable method of defining the stress distribution in polyethylene elements in both, hip and knee joint endoprostheses.

## 2. Numerical analysis of the loads affecting the modular hip joint endoprosthesis

The geometric model was built using Autodesk Inventor Professional 2016 software. Due to the way of virtual fastening, the geometric model of the cup did not have so-called “longitudinal cuts” that counteract the rotation of the cup.

In the geometrical model presented in Fig. 1, the diameter of a real polyethylene cup and head of the hip joint endoprosthesis was  $\phi$  32 mm. In the stem section, a part closer to the modular set was based on widely applied solutions [9].



Fig. 1. Geometric model of hip prosthesis

The numerical analysis was performed by means of the finite elements method using Autodesk Simulation Mechanical 2016 software. The spatial system of restraint and load based on identifying movement loads in hip joint, created by Bergman & Będziński and was modified and simplified for the purpose of the simulation. The values of loads were assumed on the basis of the literature data [10, 11, 12, 13].

The following values were adopted:

$P_1 = 700$  N – load resulting from a patient’ weight,

$P_2 = 50$  N – load resulting from the work of muscles.

The spots of loads are depicted on the Figure 2.

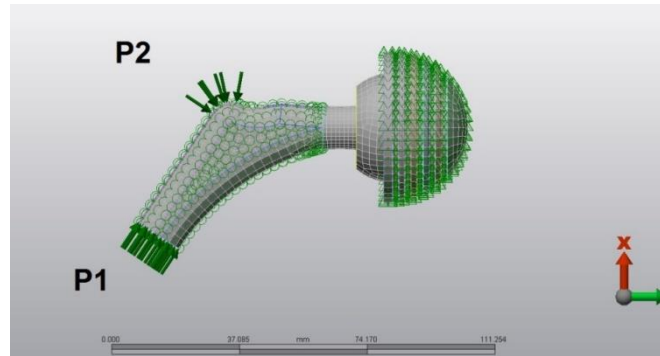


Fig. 2. Model of the loads affecting the analyzed system

The movement of the head around the cup, with a friction coefficient  $\mu = 0.2$ , was modeled. However, the presented static analysis does not include considerations in this respect.

Following material combinations were analyzed:

- stem Ti6Al4V, head Al<sub>2</sub>O<sub>3</sub>, cup UHMWPE (Ultra High Molecular Weight Polyethylene),
- stem Ti6Al4V, head CoCrMo, cup UHMWPE,
- stem Ti6Al4V, head Ti6Al4V, cup UHMWPE.

The mechanical parameters of these materials are presented in Table 1.

Table 1. Mechanical features of biomaterials

Element of the model	Young's module [MPa]	Poisson's coefficient $\nu$
Alloy CoCrMo	$2.0 \times 10^5$	0.3
Alloy Ti6Al4V	$1.1 \times 10^5$	0.3
UHMWPE	$1.0 \times 10^3$	0.4
Ceramics Al <sub>2</sub> O <sub>3</sub>	$3.8 \times 10^5$	0.22

Figures 3-5 present examples of stress, strain and displacement distribution in the analyzed models.

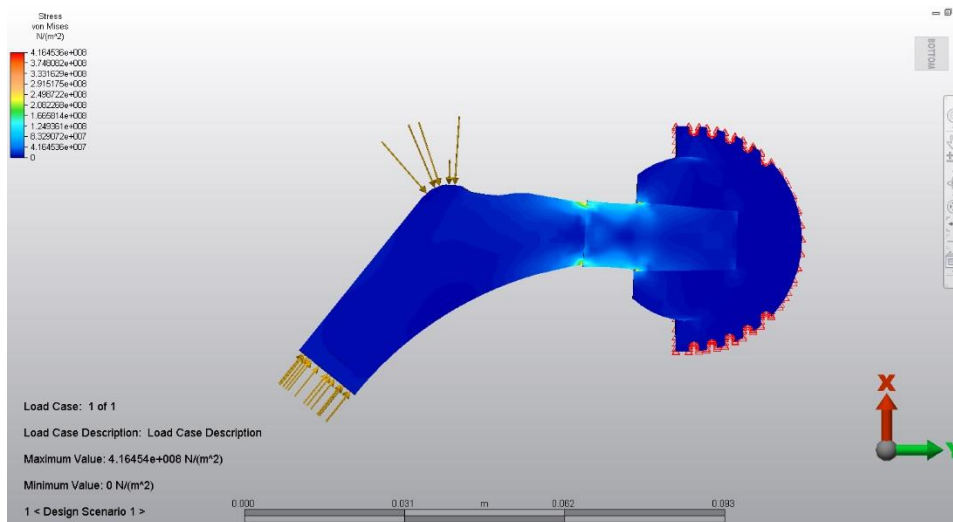


Fig. 3. Stress distribution for the combination: stem – Ti6Al4V, head – Al<sub>2</sub>O<sub>3</sub>, cup UHMWPE

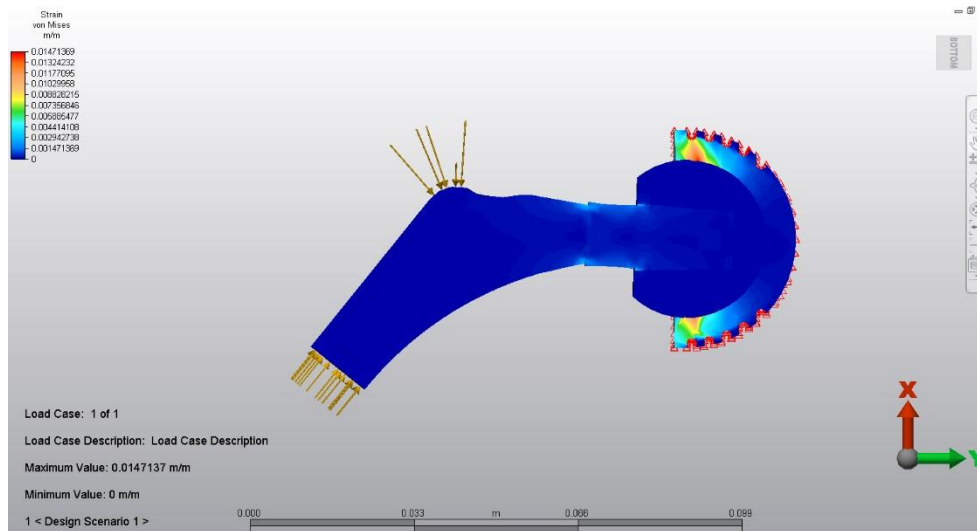


Fig. 4. Strain distribution for the combination: stem – Ti6Al4V, head – CoCrMo, cup UHMWPE

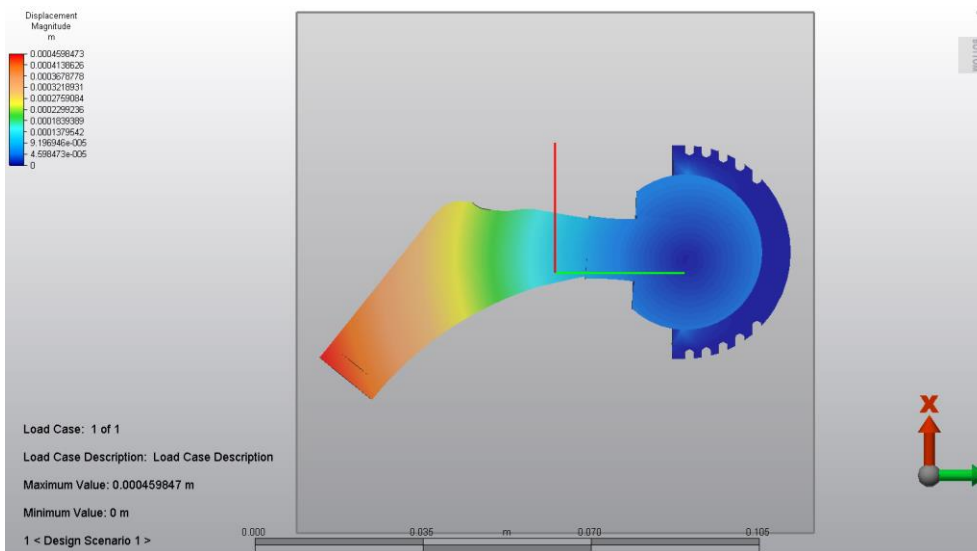


Fig. 5. Displacement distribution for the combination: stem – Ti6Al4V, head – Ti6Al4V, cup UHMWPE

Figure 6 illustrates maximal stresses determined in the examined configurations. The highest values of stresses were observed for the combination: stem – Ti6Al4V, head – Al<sub>2</sub>O<sub>3</sub>, cup UHMWPE, with the maximum value at the level of 416 MPa. Lower values (408 MPa) were obtained for the combination: stem – Ti6Al4V, head – CoCrMo, cup UHMWPE; while the lowest (391 MPa) – for the: stem – Ti6Al4V, head – Ti6Al4V, cup UHMWPE. The concentration of the stresses in all the cases was placed in the area of contact of the endoprosthesis stem with its head. It should be noted that it is a modular endoprosthesis, and therefore there is a contact between the tapered surface of the stem and the internal part of the opening in the head.

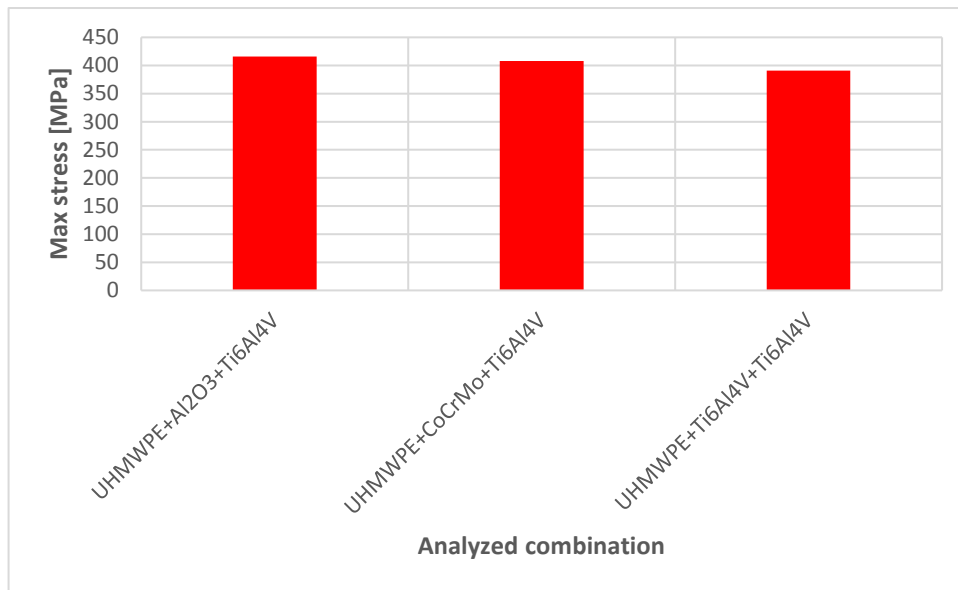


Fig. 6. Values of the maximal stresses

### 3. Numerical models of knee joint endoprostheses

The numerical models are simplified versions of the original endoprostheses, though the sleds' geometry has been maintained. This approach enables to keep the general shape of the endoprostheses and to imagine the strain distribution on the insert's surface [14, 15].

The Figure 7 presents the simplified sled models.

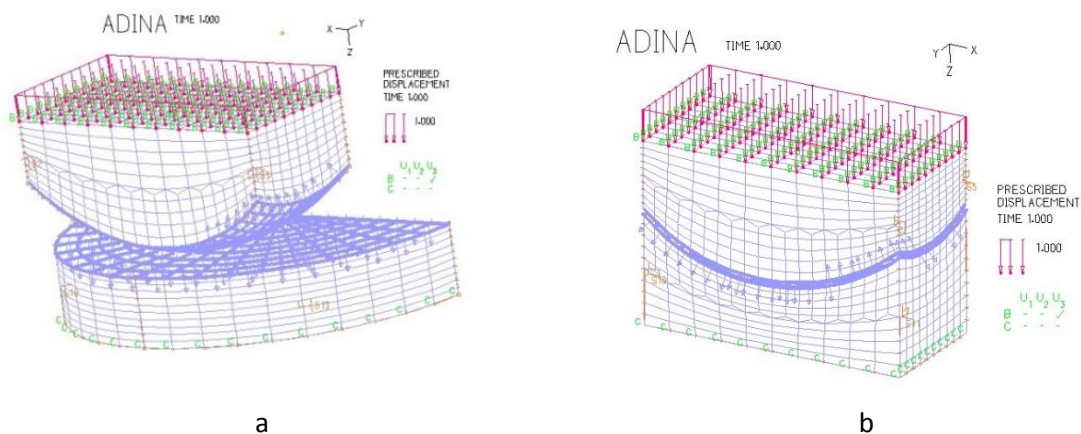


Fig. 7. Simplified sled models used for calculations: a) endoprosthesis with flat insert, b) endoprosthesis with spherical insert

The main purpose of the calculations was to define stress distribution on the surface of the polyethylene insert and directly underneath. Three heights of polyethylene inserts were analyzed: 8, 13 and 22 mm, and two sleds of cross section radiuses of 17 and 27 mm, respectively.

### 4. Assumptions for calculations

The calculations were based on the following assumptions, taking into account the influence of important factors on the stress:

- the influence of cross-section radius of metal sled of endoprosthesis on the value of strain in the contact area of these elements;
- the influence of the kind of contact on the value of the strain.

Contacts between elements of endoprosthesis may be as follows:

- point contact: the loaded elements touch primarily; then the contact gradually turns into linear contact;
- surface contact: when sled works with spherical polyethylene insert [2, 4].

The elements were exposed to the load similar as the one occurring in the real knee joint. Numerical analysis was conducted with The ADINA 7.5.1. The obtained results may be used to evaluate the distribution of wear of particular areas of sleds and polyethylene inserts (flat and spherical), before they are used in endoprostheses.

## 5. Material data

The calculations were conducted for flat and spherical inserts made of medical UHMWPE of higher density and 8 mm thick. Regular load for endoprostheses is 1500 N. The calculations considered two different geometrical sleds: of 17 mm and 27 mm cross-section radiiuses.

It was assumed that all materials used in models (medical alloy of titanium Ti6Al4V, UHMWPE polyethylene), are linearly elastic and homogeneous. Additionally, they are isotropic with constant mechanical features. The calculations are based on regular simplified load model, where normal force is put to the upper surface of the sled.

The load applied to the numerical models was the result of the interaction between joint surface of femoral bone and implant's polyethylene insert.

The above model is simplified: (polyethylene insert is the weakest element of endoprostheses and is the most responsible for the endoprosthesis durability.

All described models were constructed in The ADINA System 7.5.1 based on The Finite Elements Method.

## 6. The analysis of the strain in the set sled – flat insert and set sled – spherical insert in the endoprosthesis

The obtained results (Figures 8-11) show the values of strains in cross- and along-section of the analysed numerical models with flat insert.

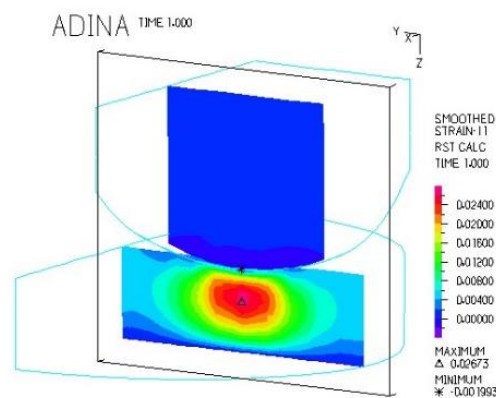


Fig. 8. Strain distribution of the material underneath the surface of flat polyethylene insert working with the metal sled. Cross-section of the model. Sled with cross radius 27 mm. Load 1500 N.

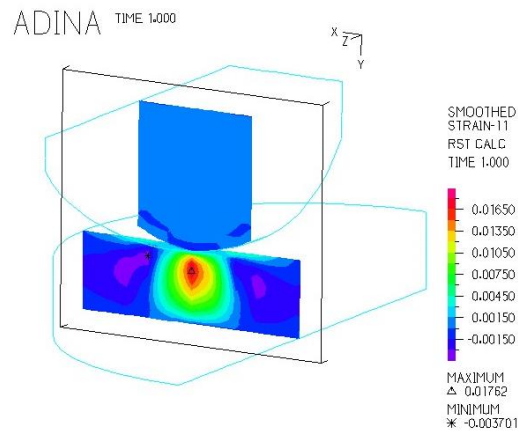


Fig. 9. Strain distribution of the material underneath the surface of flat polyethylene insert working with the metal sled. Cross-section of the model. Sled with cross radius 17 mm. Load 1500 N.

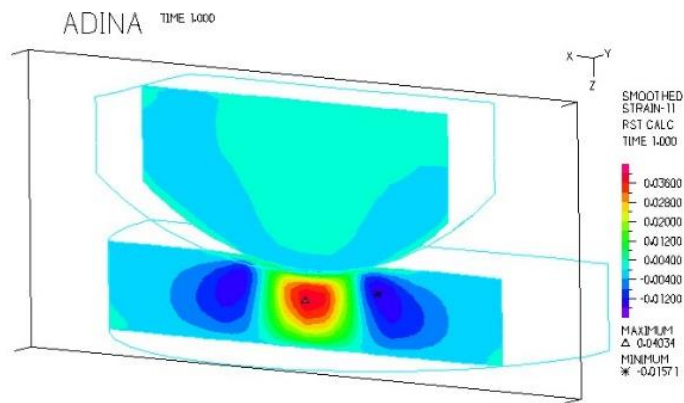


Fig. 10. Strain distribution of the material underneath the surface of flat polyethylene insert working with the metal sled. Longitudinal cross-section of the model. Sled with cross radius 27 mm. Load 1500 N.

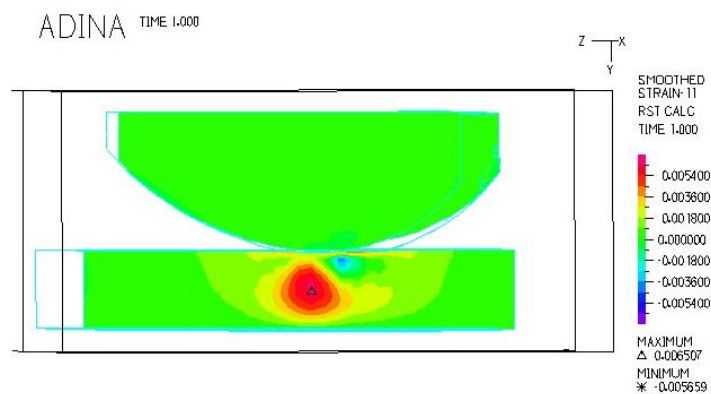


Fig. 11. Strain distribution of the material underneath the surface of flat polyethylene insert working with the metal sled. Longitudinal cross-section of the model. Sled with cross radius 17 mm. Load 1500 N.



Figures 12 to 15 show the values of strains in cross- and along-section of the analysed numerical models with spherical insert.

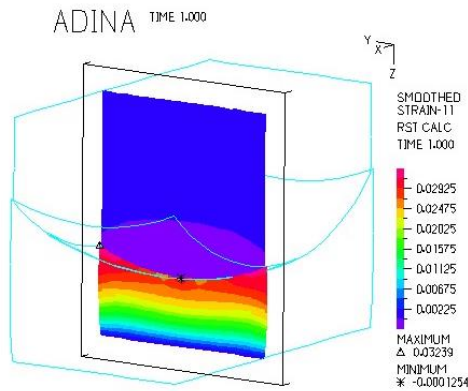


Fig. 12. Strain distribution of the material underneath the surface of flat polyethylene insert working with the metal sled. Cross-section of the model. Sled with cross radius 27 mm. Load 1500 N.

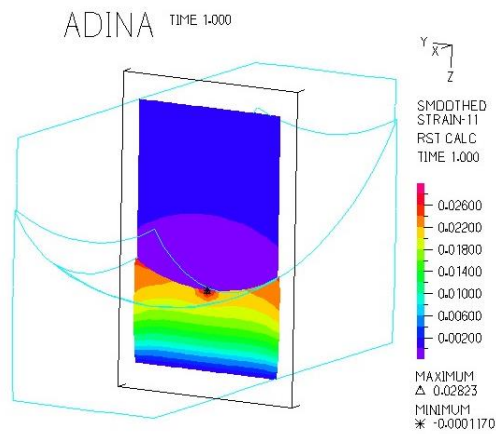


Fig. 13. Strain distribution of the material underneath the surface of flat polyethylene insert working with the metal sled. Cross-section of the model. Sled with cross radius 17 mm. Load 1500 N.

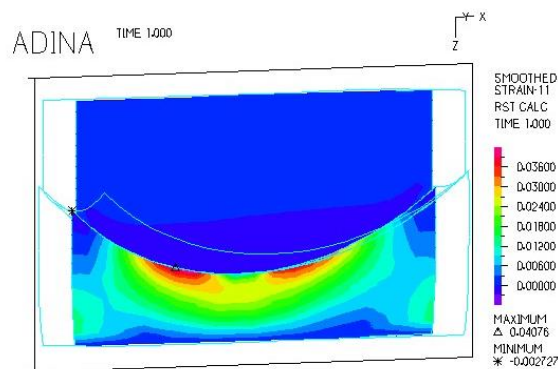


Fig. 14. Strain distribution of the material underneath the surface of flat polyethylene insert working with the metal sled. Longitudinal cross-section of the model. Sled with cross radius 27 mm. Load 1500 N.



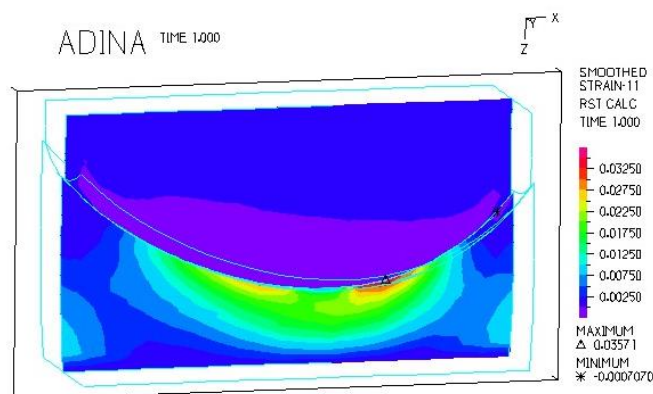


Fig. 15. Strain distribution of the material underneath the surface of flat polyethylene insert working with the metal sled. Longitudinal cross-section of the model. Sled with cross radius 17 mm. Load 1500 N.

## 7. The influence of geometry and contact area surface on the value of the strain

All the results clearly show that the strain in the endoprosthesis is concentrated in the polyethylene insert right underneath the surface where both elements are in touch.

The strain distribution is different in both kinds of inserts. The results confirmed the theory: the strain values are higher in the flat insert than in the spherical one. Additionally, in the spherical insert the distribution is more regular than the one in the flat insert. As for the influence of the cross-section radius it is clear that the sled with smaller one, 17 mm, generates higher values of the strain than the sled of 27 mm radius.

## 8. Conclusions

The conducted analysis leads to the following conclusions:

1. The highest strain occurs when UHMWPE cap works with  $Al_2O_3$  head on Ti6Al4V mandrel. The bigger strain occurs where the cone surface of the mandrel touches the internal slot of the endoprosthesis's head.
2. The highest values of deformation are observed in places where the cap touches the endoprosthesis's head. When polyethylene cap is used, less stress and strain is transferred into deeper layers of the material and most important – to the pelvis bone.
3. The analysis allows to define „weak points” of the tested solution, thus may be used to reduce the endoprosthesis's abnormal wear.
4. The contact strain values can be decreased by proper adjustment of cooperating surfaces and substituting the linear contact by the surface.
5. When the sled has 17 mm cross-section radius, the strain and stress concentration in the insert is much higher than when the radius is 27 mm. It proves that the value of cross-section radius is critically important.
6. The results present the contact areas and the areas of highest values of strain, and the print-points of metal elements in the polyethylene.
7. It is critical to continue the analysis of the proposed model in order to complete it with additional examination including a contact with bone.
8. It is advised to conduct the tests on the influence of the change of materials' parameters on the stresses in the modelling conditions.

## REFERENCES

- [1] M. Gierzyńska-Dolna: *Odporność na zużycie materiałów stosowanych na endoprotezy*, Mechanika w Medycynie, Rzeszów 1996, s. 131–141.

- [2] E. Andrysewicz, J.R. Dąbrowski: *Zagadnienia oceny właściwości użytkowych tworzyw sztucznych do zastosowań w ortopedii*, Inżynieria Biomateriałów, vol. 5–6, s. 3–8.
- [3] Ch.F. Scifert, T. Brown, J. Lipman: *Finite element analysis of a novel design approach to resisting total hip dislocation*, Clinical Biomechanics, vol. 14, 1999, s. 697–703.
- [4] A.M. Ryniewicz, T. Madej: *Analiza naprężeń i przemieszczeń w strefie roboczej endoprotezy stawu biodrowego*, Mechanika w Medycynie, vol. 6, 2002, s. 127–134.
- [5] A.M. Ryniewicz, T. Madej: *Preclinical tests of endoprostheses of hip joint using finite element methods*, Engineering of biomaterials, vol. XIII(94), s. 14–23.
- [6] S. Singha, A.P. Harshaa: *Analysis of Femoral Components of Cemented Total Hip Arthroplasty*, Journal of The Institution of Engineers, Ser. D, 2015, doi:10.1007/s40033-015-0096-2.
- [7] El-Shiekh, F. Hussam El-Din: *Finite element simulation of hip joint replacement under static and dynamic loading*, PhD thesis, Dublin City University, 2002.
- [8] A. John, P. Orantek: *Symulacja oddziaływań dynamicznych w stawie biodrowym ze sztuczną panewką*, Modelowanie inżynierskie, vol. 32, 2006, s. 211–218.
- [9] Medgal implant i instrumentaria ortopedyczne, <http://www.medgal.com.pl/pl,ms-produkty-0-0-produkty.html>
- [10] R. Będziński: *Biomechanika inżynierska*, Oficyna Wydawnicza Politechniki Wrocławskiej, Wrocław 1997.
- [11] T. Madej, A. Ryniewicz: *Modelowanie i symulacje wytrzymałościowe w stawie biodrowym zaopatrzone protezą nakładkową jako procedura diagnostyczna przed zabiegiem kapoplastyki*, Tribologia, nr 2, 2013.
- [12] M. Gierzyńska-Dolna: *Tribologia*, Wydawnictwo Politechniki Częstochowskiej, Częstochowa 2002.
- [13] A. Bednarek, P. Zakrzewski, W. Parol: *Proteza nasadowa (modularna) stawu biodrowego Metha – założenia biomechaniczne, wczesne wyniki kliniczne*, IV Międzynarodowe Sympozjum Koksartozu, 8–10.05.2008, Katowice.
- [14] A.M. Ryniewicz, A. Ryniewicz: *Analiza mechanizmu smarowania stawów człowieka w badaniach in vitro oraz in vivo*, Przegląd elektrotechniczny, vol. 90(5), 2014, s. 142–145.
- [15] M. Gierzyńska-Dolna, J. Kubacki, A. Wieczorek, K. Tatar, *Mechanizm zużycia endoprotezy saneczkowej stawu kolanowego*, Biology of Sport, 1998, s. 112–119.

otrzymano / submitted: 24.10.2016  
proprawiona wersja/ revised 26.07.2017  
zaakceptowano / accepted: 30.09.2017